Computers and Chemical Engineering 104 (2017) 311–322

Contents lists available at ScienceDirect

Computers and Chemical Engineering

journal homepage: www.elsevier.com/locate/compchemeng

A pharmacokinetic/pharmacodynamic model of ACE inhibition of the renin-angiotensin system for normal and impaired renal function

Ashlee N. Ford Versypt*, Grace K. Harrell, Alexandra N. McPeak

Department of Chemical Engineering, Oklahoma State University, Stillwater, OK 74078, USA

ARTICLE INFO

Article history:
Received 16 January 2017
Received in revised form 14 March 2017
Accepted 19 March 2017
Available online 25 April 2017

Keywords:
Nonlinear dynamic modeling
Parameter estimation
Systems pharmacology
Hypertension
Chronic kidney disease

ABSTRACT

Angiotensin II (Ang II) is a hormone that regulates blood pressure and is produced by the renin-angiotensin system (RAS). Angiotensin converting enzyme (ACE) inhibitor drugs inhibit the production of Ang II. ACE inhibitors are well-characterized for use in hypertension, but they are not as well understood for use in chronic kidney disease. Existing models for ACE inhibitors have only been applied to normal renal function. Here, published experimental data for two ACE inhibitors (benazepril and cilazapril) in patients with normal and impaired kidneys are used to construct a pharmacokinetic model of the fate of drug doses in the circulatory system. A pharmacodynamic model connecting drug concentration to the inhibition of the RAS and production of Ang II is proposed and parameterized for the two drugs in the cases of normal and impaired renal function. The model is packaged as a MATLAB app to facilitate reuse for research and educational purposes.

1. Introduction

Angiotensin II (Ang II) is a hormone that regulates the blood pressure by constricting the blood vessels. A sustained high level of Ang II leads to hypertension, which increases the work required for the heart to pump blood through the body and causes numerous health problems. Angiotensin converting enzyme (ACE) inhibitors are a class of pharmaceuticals that inhibit the production of Ang II from angiotensin I (Ang I), thereby reducing the Ang II concentration and thus lowering the blood pressure. The conversion of Ang I to Ang II is a crucial step in the biochemical reaction network called the renin-angiotensin system (RAS) (Fig. 1). Ang II concentration has a negative feedback effect on the production of renin, which catalyzes the upstream production of Ang I from angiotensinogen (AGT). Here, we consider the subset of the RAS reaction network that includes the hormones and the enzymes affected directly by ACE inhibition (Fig. 1).

ACE inhibitors are known to aid patients with hypertension, congestive heart failure, and chronic kidney disease (CKD) (Balfour and Goa, 1991; Brown and Vaughan, 1998; Corbo et al., 2016). CKD is a severe complication of diabetes and a significant factor leading to morbidity and mortality in both type I and type II diabetic patients. CKD is the primary cause for end-stage renal disease and can lead to kidney failure if Ang II is not regulated. It is important to slow the rate of progression of CKD before irreversible kidney damage occurs, and ACE inhibitors have been shown to be effective at doing so (Asher and Murray, 1991; Hoyer et al., 1993; Brown and Vaughan, 1998; Hsu, 2014; Yamout et al., 2014). As both diabetes and chronic kidney disease are comorbidities of hypertension, ACE inhibitors are particularly attractive pharmaceuticals for targeting multiple indications simultaneously.

Many ACE inhibitor pharmaceuticals are on the market. The ACE inhibitors benazepril and cilazapril are selected for this study because both are renoprotective and used to treat CKD and hypertension (Hoyer et al., 1993; Niu et al., 2014). Also, studies have been conducted to collect data on benazepril and cilazapril drug dose and effects on the RAS for hypertensive human patients with normal renal function (NRF) and impaired renal function (IRF) (Shionoiri et al., 1988, 1992; Kloke et al., 1996). The model and parameter estimation techniques in the present work could be readily adapted for other ACE inhibitor drugs if pharmacokinetic and pharmacodynamic experimental studies have been performed to characterize the actions of those drugs. Note that benazepril and cilazapril are both extensively bioactivated to diacid chemical forms, as is common for most ACE inhibitors (Hoyer et al., 1993; Toutain and Lefebvre, 2004; LeBlanc et al., 2006). Therefore, all parameters and calculations involving either drug only use the pharmacologically active diacid form of the corresponding drug.

* Corresponding author at: 420 Engineering North, Oklahoma State University, Stillwater, OK 74078, USA.
E-mail address: ashleefv@okstate.edu (A.N. Ford Versypt).

http://dx.doi.org/10.1016/j.compchemeng.2017.03.027
0098-1354/

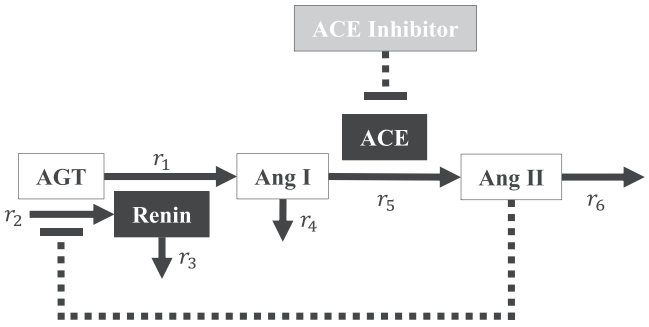

Fig. 1. The reaction network for the renin-angiotensin system. The hormones angiotensinogen (AGT), angiotensin I (Ang I), and angiotensin II (Ang II) are shown in the white boxes. The enzymes renin and angiotensin converting enzyme (ACE) are shown in the black boxes. The ACE inhibitor drug is shown in a gray box. The solid arrows denote the chemical reactions, and the dotted lines denote the inhibitory signals. $r_1, r_2, \ldots, r_6$ are the labels for the reactions.

Several previous mathematical models have been developed that focus on the physiological mechanisms of blood pressure regulation in healthy patients in the absence of pharmaceutical interventions (Guyton et al., 1972; Karaaslan et al., 2005; Guillaud and Hannaert, 2010; Arciero et al., 2015; Ford Versypt et al., 2015). A relatively small number of models have been proposed that consider the pharmacokinetics (PK) and pharmacodynamics (PD) of ACE inhibitors and their effects on blood pressure or Ang II concentrations (Toutain and Lefebvre, 2004; Hong et al., 2008; Lo et al., 2011; Ramusovic and Laeer, 2012; Claasen et al., 2013). We briefly review the highlights of each of these models in the following paragraph.

Toutain and Lefebvre (2004) developed a physiologically-based PK model for ACE inhibitor disposition in dogs and cats. The model considered the dynamics of binding of an ACE inhibitor specifically and nonspecifically to blood and tissue components and the elimination of the unbound ACE inhibitor. The PK model was coupled to the PD model by use of a Hill function for predicting the efficacy of the measured plasma ACE activity subject to inhibition. The effects of changes in the ACE activity on the RAS cascade were described but not quantified by the model. Hong et al. (2008) created a PK/PD model of renin inhibition, which is similar to ACE inhibition but it impedes r_1 in Fig. 1 instead of r_5. The model considered one-, two-, and three-compartment models to describe the PK of a renin inhibitor drug. They included a periodic time-dependent baseline renin production rate and the feedback of Ang II concentration on renin production through a Hill function. Another Hill function was included for connecting the drug concentration to the PD model. They used a linear correlation to relate plasma renin activity and renin concentration and provided a citation to evidence supporting that this correlation is valid under physiological conditions. The Ang II concentration was treated as a linear function of the Ang I concentration, which changed in response to renin inhibition. Lo et al. (2011) proposed a model of hypertension focusing on the RAS pathway. They adapted the classic Guyton and Karaaslan models (Guyton et al., 1972; Karaaslan et al., 2005) for blood pressure regulation and incorporated the biochemical reaction network of the RAS. The detailed model was parameterized for a representative normotensive virtual patient. Feedback between the downstream products of Ang II and renin was incorporated into the model. Three types of RAS-modulating pharmaceutical therapies including ACE inhibitors were explored. The model did not include an explicit representation of the PK for any of the three types of therapies. Instead, single terms in the PD model are adjusted in a manner not explicitly tied to the dosing magnitudes or schedules. E.g., ACE inhibitors were considered by changing the value of the rate constant for the conversion of Ang I to Ang II (reaction r_5 in Fig. 1). They also considered a renal-specific model for the local RAS in the renal vascular and tissue compartments. Ramusovic and Laeer (2012) created a PK/PD model for ACE inhibitors, angiotensin receptor blockers, and renin inhibitors. A Hill function was used for the inhibition effect of the ACE inhibitor on the Ang II production rate. Another Hill function was used for the feedback of Ang II on the renin production using the absolute magnitude of the Ang II concentration. PRA was treated as a linear function of Ang I. Their model predicted steeper Ang I increases and Ang II reductions resulting from ACE inhibition than those that were observed in the data for two different dosing schemes for benazepril in normal renal function. Claasen et al. (2013) proposed a physiologically-based PK/PD model for ACE inhibition that explicitly considered the expression of ACE in 15 organs throughout the body. Different physiological parameters were obtained from the PK-Sim software for multiple populations and data sets. Enalapril was selected as the ACE inhibitor in the study. Binding of the drug to ACE was implemented in the plasma compartment of each organ, thus connecting the PK and PD portions of the model. The PD model for the RAS network included competitive inhibition of the secretion of renin by Ang II. In regards to CKD, a significant drawback of the existing ACE inhibitor PK/PD models, with the exception of Lo et al. (2011), is that these models have considered only healthy or hypertensive human and veterinary patients with normal renal function. Lo et al. (2011) did consider impaired renal function in their model, but the PK/PD of specific ACE inhibitors of different doses cannot be readily calculated from their model.

The primary aim of this study is to fill the gap in PK/PD models by developing such a model specifically for ACE inhibition in impaired renal function, given the prevalence of using this class of pharmaceuticals for treating CKD. A secondary aim is to develop a straightforward model that can determine biomarker concentrations in good agreement with experimental data while also being fast and easy to use. A challenge with using or adapting the existing models is that some are very physiologically detailed and difficult to reproduce or extend to the impaired renal function case. For example, the model by Guillaud and Hannaert (2010) was developed for physiological blood pressure regulation by the RAS in normal renal function. The model has a negative feedback loop for renin production that involves complicated expressions dependent on physiological processes that are not easily quantified for the impaired renal function case considered here.

In the following sections, we define a model for the pharmacokinetic chemical reactions involved in the natural production of Ang II and the pharmacodynamic physiological response to ACE inhibitors in a time and dose-dependent manner for both normal and impaired renal function. We describe the numerical techniques to solve the equations in MATLAB, the methods for fitting parameters to data, and the development of a MATLAB graphical user interface (GUI). We present the results for global and local sensitivity analyses and for several validation case studies. Together, the model, the parameter sets, and the GUI satisfy the aims of the study.

2. Methodology

2.1. Data extraction

Experimental data used in this paper are extracted from graphs in the original sources, which are referenced in the text, using the open-source Java program Plot Digitizer (SourceForge, 2015).

2.2. Pharmacokinetic model

Pharmacokinetics describes the movement of a drug into, through, and out of the body via the processes of absorption,

Table 1
Pharmacokinetic parameter values for benazepril (Shionoiri et al., 1992) and cilazapril (Shionoiri et al., 1988) for normal renal function (NRF) and impaired renal function (IRF).

Parameter	Units	Benazepril		Cilazapril	
		NRF	IRF	NRF	IRF
Reported in the literature					
$t_{1/2}$	h	5.2	20.1	8.4	7.3
t_{max}	h	1.5	2.4	3.2	4.3
AUC	ng h ml^{-1}	528.6	1358	226.8	583.4
Calculated from literature values					
k_e	h^{-1}	0.866	0.034	0.083	0.095
k_a	h^{-1}	2.193	1.645	0.787	0.464

distribution, metabolism, and excretion following the administration of the drug. The typical one-compartment model with first-order absorption from the site of administration and first-order elimination is used here for the oral administration of an ACE inhibitor drug. This model assumes that the drug (either benazepril or cilazapril) enters the circulatory system at a rate proportional to the amount of drug remaining to be absorbed from the digestive system. The change in drug concentration in the blood plasma, C_D, over time, t, for a single dose is described by (Dhillon and Kostrzewski, 2006; Byers and Sarver, 2009)

$$\frac{dC_D}{dt} = k_a F d \exp(-k_a t)/V - k_e C_D \tag{1}$$

where k_a is the absorption rate constant, F is the fraction absorbed, d is the dose size, V is the volume of distribution, and k_e is the elimination rate constant. The initial drug concentration before the first dose is $C_D(0) = 0$.

By superimposing the single dose solutions to (1) for multiple doses over time, the concentration of the drug in the body resulting from repeated dosing at uniform time intervals is (Byers and Sarver, 2009)

$$C_{D,n}(t') = \frac{k_a F d}{(k_a - k_e)V} * \left(\frac{1-\exp(-nk_e\tau)}{1-\exp(-k_e\tau)} \exp(-k_e t') - \frac{1-\exp(-nk_a\tau)}{1-\exp(-k_a\tau)} \exp(-k_a t') \right) \tag{2}$$

where $C_{D,n}(t')$ is the drug concentration after the nth dose for $n = 1, 2, \ldots, N$, t' is the time since the most recent dose, and τ is the time interval between doses. Note that $t' = t - \tau(n-1)$ and $0 \le t' \le \tau$. After the Nth (final) dose, $C_{D,N}(t')$ is valid for $t' \ge 0$.

The PK parameters for the elimination half-life of the drug, $t_{1/2}$, the time corresponding to the maximum concentration achieved by a single dose, t_{max}, and the integrated area under the curve of drug concentration vs. time for 24 h after dosing, AUC, are useful for calculating the parameters, k_e, k_a, and V/F, which are required to evaluate (2) for a given dose amount and dosing interval. The values of $t_{1/2}$, t_{max}, and AUC reported in the literature for single doses of the diacid forms of benazepril and cilazapril for NRF and IRF are given in Table 1.

The definition of the elimination half-life of the drug is used to determine k_e by

$$k_e = \frac{\ln(2)}{t_{1/2}} \tag{3}$$

The time at which the maximum concentration is reached for a single dose is related to k_a and k_e by (Byers and Sarver, 2009)

$$t_{max} = \frac{\ln(k_a/k_e)}{k_a - k_e} \tag{4}$$

Table 2
Inhibition parameter values for benazepril (Shionoiri et al., 1992) and cilazapril (Shionoiri et al., 1988).

Parameter	Units	Benazepril	Cilazapril
$C_{D_{50}}$	ng ml^{-1}	2.20	3.61
m	–	0.99	1.19

The root of (4) gives the value of k_a. The ratio V/F is found using the area under the curve, AUC, in the general relationship (Byers and Sarver, 2009)

$$\frac{V}{F} = \frac{d}{k_e \text{AUC}} \tag{5}$$

Because V/F is dose dependent, the calculated value is not shown in Table 1, while the values for k_e and k_a are shown.

2.3. Pharmacodynamic model

Pharmacodynamics describes what the drug does to the body including the mechanism of drug action and the relationship between the drug concentration and the effect. PD, in combination with PK, helps explain the relationship between dose and response.

As is common for PD models, a Hill function is used to fit the relationship between the drug concentration and the extent of ACE inhibition (Shionoiri et al., 1992, 1988)

$$I = \frac{100 C_D^m}{C_{D_{50}}^m + C_D^m} \tag{6}$$

where I is the observed inhibition percentage, $C_{D_{50}}$ is the drug concentration that yields 50 percent inhibition, and the power term, m, accounts for the degree of sigmoidicity in the relationship. The ACE inhibition parameter values found in the literature for the diacid forms of benazepril and cilazapril are shown in Table 2. Note that no differences in these parameters were reported for NRF vs. IRF.

The PD model also includes the net rates of formation of Ang I, Ang II, and renin in terms of concentrations assuming that the volume of distribution is constant. The concentrations for the species are denoted as C_{AI}, C_{AII}, and C_R for Ang I, Ang II, and renin, respectively. Each reaction that contributes to the generation or consumption of Ang I, Ang II, and renin is labeled as r_i for $i = 1, 2, \ldots, 6$ in Fig. 1. In the model for the reaction network, the term "baseline" or the initial condition refers to the corresponding concentration level or reaction rate in the absence of the drug for $t \le 0$. The initial concentrations are denoted as $C_{AI}(0)$, $C_{AII}(0)$, and $C_R(0)$.

The first reaction is the production of Ang I from AGT catalyzed by renin. The reaction rate in terms of deviations from the baseline is defined as

$$r_1 = B_{AI} + k_R(C_R - C_R(0)) \tag{7}$$

where B_{AI} is the baseline production of Ang I and k_R is the catalytic rate constant for renin. The first-order dependence on C_R is consistent with Michaelis-Menten kinetics where the enzyme concentration has a first-order effect. The substrate AGT concentration is assumed to be unaffected by ACE inhibition.

The second reaction is the production of renin. The reaction rate has two contributions: the baseline production of renin without feedback, B_R, and the feedback inhibition of Ang II on the production of renin, which is given as a logistic function dependent on deviations in C_{AII},

$$r_2 = B_R + k_f (C_{AII}(0) - C_{AII}) \left(1 - \frac{C_{AII}(0) - C_{AII}}{f}\right) \tag{8}$$

where k_f is the feedback rate constant and f is the feedback capacity. The logistic function in (8) represents the capacity that Ang II deviations have to impact renin through the negative feedback

mechanism. Decreases in C_{AII} compared to the baseline increase renin production (the dominant case for ACE inhibition) and vice versa. As deviations in Ang II become large, i.e., for low C_{AII}, the deviations approach the feedback capacity where the effective change in renin from feedback becomes saturated as there is an upper limit to the physiological secretion rate of renin.

The third reaction is the degradation of renin, which has a reaction rate of

$$r_3 = \frac{\ln(2)}{t_{1/2,R}} C_R \tag{9}$$

where $t_{1/2,R}$ is the half-life of renin.

The fourth reaction is the degradation of Ang I, which has a reaction rate

$$r_4 = \frac{\ln(2)}{t_{1/2,AI}} C_{AI} \tag{10}$$

where $t_{1/2,AI}$ is the half-life of Ang I.

The fifth reaction is the enzymatic conversion of Ang I to Ang II by ACE. The reaction rate involves inhibition of ACE by the drug and is related to the inhibition percentage from (6) by

$$I/100 = \frac{r_5|_{I=0} - r_5|_{I\geq 0}}{r_5|_{I=0}} = 1 - \frac{r_5|_{I\geq 0}}{r_5|_{I=0}} \tag{11}$$

where $r_5|_{I\geq 0}$ is the inhibited reaction rate and $r_5|_{I=0}$ is the reaction rate without inhibition or simply the Michaelis-Mention equation:

$$r_5|_{I=0} = \frac{V_{\max} C_{AI}}{K_M + C_{AI}} \tag{12}$$

where $V_{\max}$ is the maximum rate of reaction for the constant total enzyme concentration and K_M is the Michaelis constant. By substitution of (12) into (11), the reaction rate is

$$r_5 = r_5|_{I\geq 0} = \frac{V_{\max} C_{AI}}{K_M + C_{AI}} \left(1 - I/100\right) \tag{13}$$

Finally, the sixth reaction is the conversion of Ang II to downstream products by degradation, binding to receptors, and enzymatic reactions. The net reaction is considered to be due to baseline and variable levels of consumption of Ang II with linear dependence on Ang II:

$$r_6 = B_{AII} + k_{AII}(C_{AII} - C_{AII}(0)) \tag{14}$$

where B_{AII} is the baseline consumption rate for Ang II and k_{AII} is the rate constant for net consumption of Ang II.

The net rates of reaction for the variable concentrations of the hormones Ang I and Ang II and the enzyme renin are

$$\frac{dC_{AI}}{dt} = r_1 - r_4 - r_5, \tag{15}$$

$$\frac{dC_{AII}}{dt} = r_5 - r_6, \tag{16}$$

and

$$\frac{dC_R}{dt} = r_2 - r_3, \tag{17}$$

respectively. The initial conditions for the concentrations of the species are set to the reported initial values in Shionoiri et al. (1988, 1992) divided by the molecular weight of the species and converted to units of pM. The initial conditions are tabulated in Table 3. The values used for the molecular weights, $M_{w,AI}$, $M_{w,AII}$, and $M_{w,R}$, are listed in Table 4.

2.4. Plasma renin activity correlation

The concentration of renin, C_R, is tracked by (17). Shionoiri et al. (1992) reported both plasma renin concentration and plasma renin activity (PRA). However, Shionoiri et al. (1988) only reported PRA.

Table 3
Initial conditions for benazepril (Shionoiri et al., 1992) and cilazapril (Shionoiri et al., 1988) for normal renal function (NRF) and impaired renal function (IRF).

Parameter	Units	Benazepril		Cilazapril	
		NRF	IRF	NRF	IRF
$C_{AI}(0)$	pM	369	440	22.7	175
$C_{AII}(0)$	pM	16.5	20.5	11.2	29.0
$C_R(0)$	pM	0.206	0.323	0.320	1.76

Table 4
Renin-angiotensin system parameter values.

Parameter	Units	Value	Source
$M_{w,AI}$	kDa	1.3	Wang et al. (2012)
$M_{w,AII}$	kDa	1.05	Noda et al. (2006)
$M_{w,R}$	kDa	48	Morimoto et al. (1980)
$t_{1/2,AI}$	min	0.5	van Kats et al. (1997)
$t_{1/2,R}$	min	15	Oates et al. (1974)

Therefore, it is desireable to calculate PRA from C_R to compare predicted PRA to measured PRA values for the two data sets during parameter estimation. The concatenated NRF and IRF values of PRA and C_R for benazepril are fit to a linear function as the correlation between PRA and C_R:

$$\text{PRA} = p_1 C_R + p_2. \tag{18}$$

2.5. Numerical methods

The equations for the PK/PD model are solved simultaneously. The root of (4) is found using the function fzero in MATLAB. The ode45 function in MATLAB for the explicit Runge-Kutta-Fehlberg method is used to solve the system of ordinary differential equations with absolute tolerance set to 10^{-6} and the relative tolerance set to 10^{-12}. The time step is set adaptively by ode45, but the time step is constrained to a maximum value of $\tau/500$, where τ is the dosage interval (typically once daily or $\tau = 24$ h). Confidence intervals are determined by standard statistical techniques applied to the solution distributions, which are approximated as Gaussian by kernel density estimation implemented with the Kernel Density Estimation Toolbox for MATLAB (Ihler, 2003).

2.6. Parameter estimation

Several parameters are needed to solve (7)–(10) and (13)–(17). The half-lives for Ang I and renin have been measured experimentally and reported in the literature (van Kats et al., 1997; Oates et al., 1974). The values for $t_{1/2,AI}$ and $t_{1/2,R}$ are listed in Table 4. The baseline rates, B_{AI}, B_{AII}, and B_R, are determined by assuming that the initial concentrations from measurements in pharmaceutical drug studies were taken at steady-state, basal levels before the drug was administered ($t \leq 0$). Therefore, the net rates of production of Ang I, Ang II, and renin are set equal to zero in (15)–(17), respectively. For Ang I at steady state,

$$r_1 = r_4 + r_5 \tag{19}$$

Substituting the expressions for r_1, r_4, and r_5 from (7), (10), and (13), respectively, and evaluating at $t = 0$ gives

$$B_{AI} = \frac{V_{\max} C_{AI}(0)}{K_M + C_{AI}(0)} + \frac{\ln(2)}{t_{1/2,AI}} C_{AI}(0) \tag{20}$$

For Ang II at steady state,

$$r_5 = r_6 \tag{21}$$

Substituting the expressions for r_5 and r_6 from (13) and (14), respectively, and evaluating at $t = 0$ gives

$$B_{AII} = \frac{V_{\max} C_{AI}(0)}{K_M + C_{AI}(0)} \tag{22}$$

This simplifies the expression for B_{AI} (20) to

$$B_{AI} = B_{AII} + \frac{\ln(2)}{t_{1/2,AI}} C_{AI}(0) \tag{23}$$

For renin at steady state,

$$r_2 = r_3 \tag{24}$$

Substituting the expressions for r_2 and r_3 from (8) and (9), respectively, and evaluating at $t = 0$ gives

$$B_R = \frac{\ln(2)}{t_{1/2,R}} C_R(0) \tag{25}$$

The remaining parameters are k_R, k_f, f, $V_{\max}$, K_M, and k_{AII}. Preliminary results showed that $K_M \gg C_{AI}(0)$ suggesting that (13) simplifies to

$$r_5 \approx \frac{V_{\max}}{K_M} C_{AI} \left(1 - \mathrm{I}/100\right) \tag{26}$$

and (22) becomes

$$B_{AII} \approx \frac{V_{\max}}{K_M} C_{AI}(0) \tag{27}$$

In this case, the ratio $V_{\max}/K_M$ is estimated as one constant instead of two. Thus, the five estimated parameters are $V_{\max}/K_M$, k_R, k_f, k_{AII}, and f.

The parameters are estimated for each combination of drug and renal function type by a series of steps. First, arbitrary initial values for the parameters are given as the guesses for the lsqcurvefit function in MATLAB, which solves nonlinear data-fitting problems in the least-squares sense. The default trust region reflective algorithm is used in the lsqcurvefit function. The objective function that lsqcurvefit minimizes is the weighted sum of squared residuals (WSSR). The unweighted sum of squared residuals (SSR) is the squared 2-norm of the residuals between the data and the predicted values of the model for the output variables C_{AI}, C_{AII}, and PRA (indices $i = 1, 2, 3$) at discrete time points. WSSR incorporates a weighting factor, $\sigma_{i,j}$, into the calculation of the error:

$$WSSR = \sum_{i=1}^{3} \sum_{j=1}^{T} \frac{1}{\sigma_{i,j}^2} (y_{i,j} - f_i(P, t_j))^2 = \sum_{i=1}^{3} \sum_{j=0}^{T} \left(\frac{y_{i,j}}{\sigma_{i,j}} - \frac{f_i(P, t_j)}{\sigma_{i,j}} \right)^2 \tag{28}$$

where T is the total number of time samples for the data, $\sigma_{i,j}$ is the weighting factor of data point $y_{i,j}$ at output variable i and time t_j, and $f_i(P, t_j)$ is the model prediction of the output variable i at time t_j with parameter set P. It is important to weight the squared residuals because the three output variables are of different orders of magnitude. Without weighting, Ang I residuals would dominate SSR given the large magnitude of the C_{AI} values compared to the C_{AII} and PRA values. The weighting factor for benazepril is set to the standard deviations of the measured data, which is estimated by the heights of the error bars on the data in Shionoiri et al. (1992). The cilazapril data in Shionoiri et al. (1988) does not have error bars. As an approximation of the cilazpril data uncertainty, the mean fraction of benazepril data error (error bar height/reported measured value) for each output variable is used. This is a reasonable estimate given that the output variables were measured by the same laboratory with the same techniques. The weighting factors for cilazapril are assumed to be uniform in time $\sigma_{i,j} = \sigma_i$. For each output variable i, the weighting factor is set to the data uncertainty approximation multiplied by the mean value of the corresponding output variable for cilazapril. The main objective of this approach is to define a set of weighting factors for cilazapril that captures the magnitudes of the output variables while including some information about data uncertainty. The default objective function for lsqcurvefit is SSR instead of WSSR. This is easily modified to WSSR by giving the matrix of y/σ as ydata and having the model scale output variables by dividing by σ. The tolerances in the lsqcurvefit function are set to the default 10^{-6} for the function evaluations (i.e., 'TolFun') and for the step size of the parameter variations (i.e., 'TolX'). The lower bound for each parameter, except the feedback capacity, is set to zero. For the feedback capacity, small values of f result in large magnitude oscillations being introduced into the dynamics that are not consistent with the experimental data. Heuristically, if $f < 250$ pM, the lsqcurvefit function tends to find parameters that yield opposite trends for C_{AI} versus time although they have smaller WSSR than parameter sets with more realistic dynamics. Thus, we fix the lower bound of f at 250 pM.

The second step for our parameter estimation is to iteratively refine the initial guesses for the parameters using the fitted parameters from successive calls to the lsqcurvefit function while reducing the tolerances for the function and parameter variations gradually to 10^{-12}. Once the parameters converge to three significant figures, the parameters are labeled as the nominal values.

Because the nominal values may give a local minimum in the solution space, a Monte Carlo approach for multistart parameter estimation is next used to vary the initial guesses to 100 additional calls to the lsqcurvefit function. The tolerances are set to 10^{-6}. Latin hypercube sampling (McKay et al., 1979) is implemented using MATLAB code available from Marino et al. (2008) to sample the parameter space for the each of the fitted parameters independently, assuming uniform distribution in a range of 10-fold increase and decrease from nominal values. While it would be ideal to explore a larger range of parameter space, fold changes larger than 10-fold result in failure of the integration routine because the solution concentrations become severely negative. The Monte Carlo algorithm is implemented in parallel in MATLAB using a simple parfor loop. The final values for the fitted parameters are reported as the median values within the best-fit parameter sets along with the minima and maxima of the ranges of parameters. The best-fit parameter sets are those with WSSR within 1% of that for the single best set. This 1% threshold ensures that the WSSR of the median parameter set matches at least the first two significant figures of the single best set.

2.7. Sensitivity analysis

Two methods are used to quantify the sensitivity of the model output variables C_{AI}, C_{AII}, and PRA relative to changes in the input parameters. First, the local sensitivity is determined by varying one parameter at a time while holding the other parameters fixed. We evaluate the local sensitivity at a single time of 2 h after dosing because that is when most of the experimental data is approaching the peak effects of the dose. The local sensitivity indices are the first-order partial derivatives of the model outputs with respect to the changing model parameter P_k, which can be approximated by a difference equation given small perturbations ΔP_k to the input parameter:

$$\frac{\partial f_i}{\partial P_k} = \lim_{\Delta P_k \to 0} \frac{f_i(P_k + \Delta P_k, P_{n \neq k}) - f_i(P_k, P_{n \neq k})}{\Delta P_k} \tag{29}$$

where $f_i(P)$ is the model prediction of the output variable i at time $t = 2$ h evaluated at parameter set P. As is recommended by Zhang et al. (2015), we select $\Delta P_k = 0.001 P_k$. Therefore, we decrease each parameter in turn by 0.1% fold from the fitted value obtained by

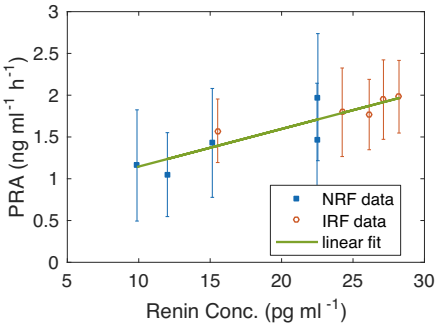

Fig. 2. Plasma renin activity (PRA) as a function of renin concentration. The benazepril data for normal renal function (NRF) and impaired renal function (IRF) were fit to a line with $R^2 = 0.79$. Data and error bars from (Shionoiri et al., 1992).

parameter estimation. The local sensitivity is normalized to remove the effects of units:

$$S_{L_{i,k}} = \frac{\partial f_i}{\partial P_k} \frac{P_K}{f_i(P_k, P_{n \neq k})} \tag{30}$$

where $S_{L_{i,k}}$ is the normalized local sensitivity index for the ith output variable and the kth parameter in parameter set P.

To account for potential interactions between parameters, a global sensitivity analysis tool is used. We adopt the eFAST method using the techniques and the MATLAB code described in Marino et al. (2008) with the default options of 5 resampling sinusoidal search curves and 65 samples per curve. The minima and maxima of the parameters are set to 10-fold, except for the lower bound of f, which is set to 250 pM as explained in the parameter estimation methods. The eFAST method generates two variance-based global sensitivity indices for each output variable i with respect to each input parameter P_k: the first-order index $S_{i,k}$ and the total-order index $S_{T_{i,k}}$. $S_{T_{i,k}}$ includes higher-order, nonlinear interactions between the P_k and the complementary set of parameters. For the global sensitivity analysis as in the local sensitivity analysis, we select the time point of 2 h after dosing for evaluating $f_i(P, t)$.

3. Results and discussion

3.1. PRA correlation

A linear fit of the combined NRF and IRF benazepril data for PRA [ng ml^{-1} h^{-1}] as a function of C_R [pg ml^{-1}] described by (18) resulted in $p_1 = 0.045$ h^{-1} and $p_2 = 0.696$ ng ml^{-1} h^{-1} with an R^2 value of 0.79. The linear fit was well within the error bars of the measurements (Fig. 2).

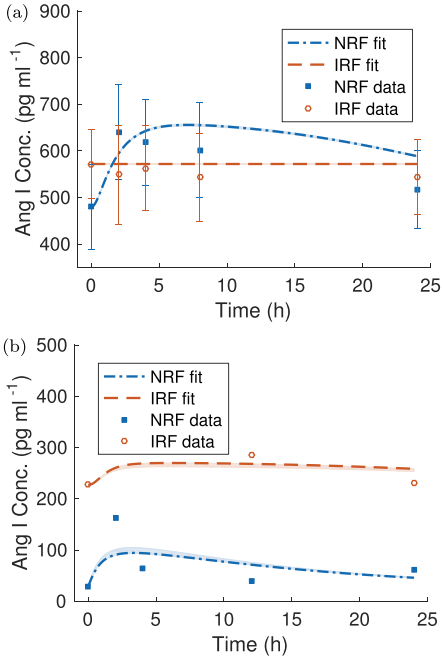

Fig. 3. Angiotensin I concentration profiles for a single dose of (a) 5 mg benazepril and (b) 1.25 mg cilazapril. Simulation results using median values from the best-fit parameter sets are shown as curves. 95% prediction confidence intervals are shaded around the curves. Symbols denote experimental data with error bars from (a) (Shionoiri et al., 1992) and (b) (Shionoiri et al., 1988).

3.2. Parameter estimation

In the experimental data used to fit the parameters, the dose for benazepril was 5 mg and that for cilazapril was 1.25 mg. The following parameters for the PD model were estimated for four cases (benazepril and cilazapril for both NRF and for IRF): V_{max}/K_M, k_R, k_f, k_{AII}, and f. The values reported for the fitted parameters were the median of the best-fit parameter sets along with the minima and maxima of the ranges of parameters (Table 5 for benazepril and Table 6 for cilazapril). The best-fit parameter sets were those with WSSR within 1% of that for the single best set (74, 93, 7, and 93 out of 101 multistart parameter sets for benazepril NRF, benazepril IRF, cilazapril NRF, and cilazapril IRF, respectively). The 95% prediction confidence intervals were determined using kernel density estimation with the best-fit parameter sets. The simulation results for the fitted parameters for all four cases are shown in Figs. 3–5 for output variables C_{AI}, C_{AII}, and PRA, respectively. Data obtained from (Shionoiri et al., 1992, 1988) are also shown in the figures.

Table 5
Estimated parameters for benazepril for normal renal function (NRF) and impaired renal function (IRF).

Parameter	Units	NRF value	NRF (min, max)	IRF value	IRF (min, max)
V_{max}/K_M	h^{-1}	1.44×10^{-2}	$(1.42, 1.47) \times 10^{-2}$	1.53×10^{-2}	$(1.52, 1.56) \times 10^{-2}$
k_R	h^{-1}	6.44×10^{4}	$(4.70, 9.44) \times 10^{4}$	1.27	$(1.13 \times 10^{-10}, 232)$
k_f	h^{-1}	6.25×10^{-2}	$(4.30, 8.20) \times 10^{-2}$	7.66×10^{-2}	$(7.50, 7.75) \times 10^{-2}$
k_{AII}	h^{-1}	6.11×10^{-1}	$(6.01, 6.23) \times 10^{-1}$	7.00×10^{-1}	$(6.94, 7.14) \times 10^{-1}$
f	pM	3.97×10^{2}	$(2.50, 24.6) \times 10^{2}$	2.50×10^{2}	$(2.50, 9.72) \times 10^{2}$

Table 6
Estimated parameters for cilazapril for normal renal function (NRF) and impaired renal function (IRF).

Parameter	Units	NRF value	NRF (min, max)	IRF value	IRF (min, max)
V_{max}/K_M	h^{-1}	1.75×10^{2}	$(1.54, 4.55) \times 10^{2}$	1.95×10^{-1}	$(1.95, 1.97) \times 10^{-1}$
k_R	h^{-1}	2.54×10^{3}	$(0.643, 4.06) \times 10^{3}$	1.81×10^{3}	$(1.33, 1.81) \times 10^{3}$
k_f	h^{-1}	3.38×10^{-1}	$(2.35, 4.18) \times 10^{-1}$	1.62×10^{-1}	$(1.61, 1.70) \times 10^{-1}$
k_{AII}	h^{-1}	2.65×10^{2}	$(2.21, 6.30) \times 10^{2}$	1.24	(1.24,1.26)
f	pM	2.79×10^{4}	$(0.272, 5.72) \times 10^{4}$	5.18×10^{5}	$(0.307, 36.1) \times 10^{5}$

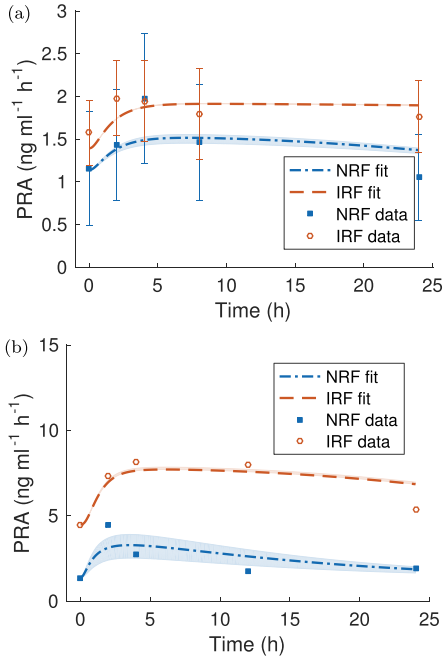

Fig. 5. Plasma renin activity profiles for a single dose of (a) 5 mg benazepril and (b) 1.25 mg cilazapril. Simulation results using median values from the best-fit parameter sets are shown as curves. 95% prediction confidence intervals are shaded around the curves. Symbols denote experimental data with error bars from (a) (Shionoiri et al., 1992) and (b) (Shionoiri et al., 1988).

The parameter sets for each case agreed well with the experimental data. In the case of benazepril with impaired renal function, the predicted C_{AI} profile was flat because the data showed a decrease in C_{AI} at early times (Fig. 4a). The model can only capture increases in C_{AI} in response to decreases in C_{AII} due to ACE inhibition. For C_{AI} and C_{AII}, the 95% confidence intervals were narrow, and

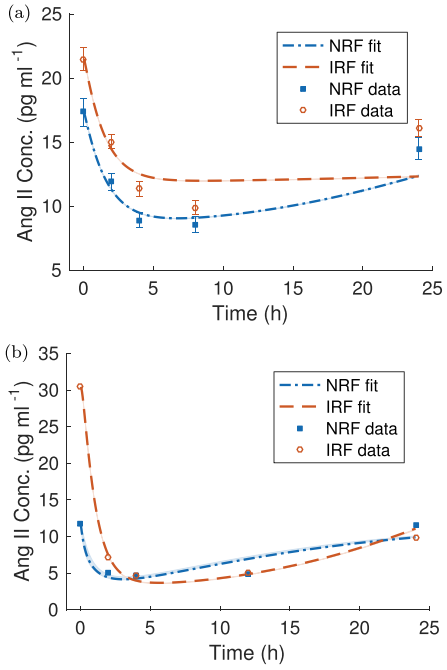

Fig. 4. Angiotensin II concentration profiles for a single dose of (a) 5 mg benazepril and (b) 1.25 mg cilazapril. Simulation results using median values from the best-fit parameter sets are shown as curves. 95% prediction confidence intervals are shaded around the curves. Symbols denote experimental data with error bars from (a) (Shionoiri et al., 1992) and (b) (Shionoiri et al., 1988).

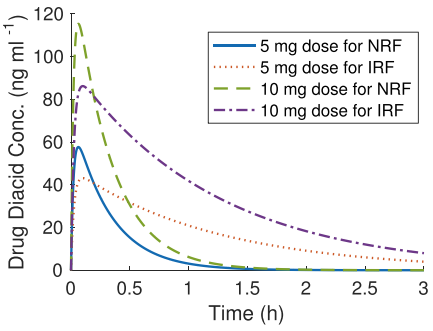

Fig. 6. Benazepril validation results: diacid form of benazepril concentration versus time after a single dose for 5 mg and 10 mg doses for NRF and IRF.

those for cilazapril were wider than those for benazepril. For PRA, the same drug-related trends were observed, but the confidence intervals were wider than for the other output variables.

3.3. Validation

Experimental data beyond those used in our parameter fitting are available in the literature for the pharmacokinetic and/or the pharmacodynamic effects of benazepril (Schaller et al., 1985; Juillerat et al., 1990; Gengo and Brady, 1991; Gismondi et al., 2015; Jiang et al., 2016) and cilazapril (Ajayi et al., 1986; Francis et al., 1987; Kloke et al., 1996), primarily for healthy volunteers or those with diabetes or hypertension with normal renal function. Additionally, several recent studies have quantified the effects of benazepril in animal models or veterinary patients with normal and impaired renal function (Brown et al., 2001; Toutain and Lefebvre, 2004; Ames et al., 2015; Sent et al., 2015; King et al., 2016; Zhang et al., 2016). However, it was challenging to compare our model predictions directly to these data as the reported Ang I initial concentrations for typical healthy volunteers or for animals were drastically different than those in the data sets we used for parameter estimation in the cases of hypertension with NRF and IRF. Additionally, some of the studies reported only the pharmacokinetic data or measured only a subset of the pharmacodynamic metrics that our model predicts or different quantities entirely, e.g., blood pressure. Therefore, we took a qualitative approach to model validation by comparing a variety of model results to a number of experimental studies for both drugs. Qualitative agreement with experimental studies as described in Sections 3.3.1 and 3.3.2 lends support to the predictive capability of the model.

3.3.1. Benazepril validation cases

For benazepril, Gengo and Brady (1991) showed that the diacid form of benazepril was significantly influenced by renal impairment, which decreases the drug elimination from the kidneys. Our simulations showed that the diacid form of benazepril maintained a measurable concentration in IRF patients for longer than 3 days (Fig. 6) just as in (Gengo and Brady, 1991).

Schaller et al. (1985) studied benazepril in normal volunteers without hypertension. They measured C_{AI}, C_{AII}, and PRA at 0, 1, 4, 8, and 24 h for doses of 2 mg, 5 mg, 10 mg, and 20 mg. They observed Ang I concentrations peaking around 8 h and increasing with dose. The Ang I levels did not return to baseline for any of the doses. They also showed that Ang II concentration dropped substantially in the first hour and that the ACE inhibitory effect on Ang II concentration lasted longer than 24 h even with the smallest 2 mg dose. Our simulation results for the same doses of benazepril as in the experimental study for NRF (Schaller et al., 1985) followed these same trends (Fig. 7).

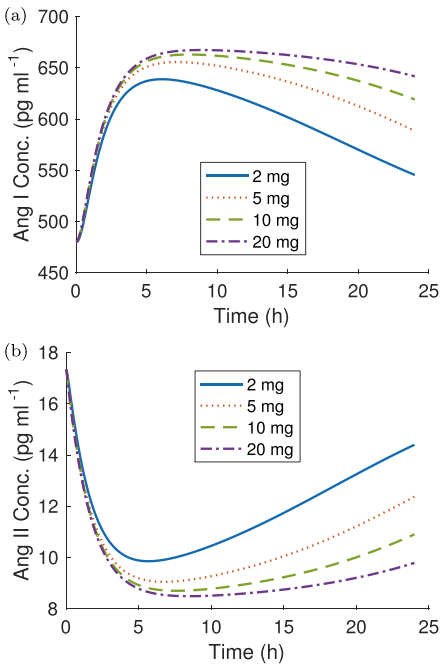

Fig. 7. Benazepril validation results for doses of benazepril for NRF: (a) Ang I concentration and (b) Ang II concentration as functions of time.

3.3.2. Cilazapril validation cases

For cilazapril, Ajayi et al. (1986) measured the percent of ACE inhibition for a placebo and 5 mg, 10 mg, and 20 mg doses of cilazapril for patients with hypertension and NRF. Their results showed that inhibition sufficiently approached the maximum inhibition at a dose of 5 mg, particularly for the first 8 h, suggesting that lower doses may be useful in practice. We repeated this experiment with cilazapril for NRF *in silico* (Fig. 8) and included the effects of a 2.5 mg dose as well. We observed that the 5 mg dose approached the inhibition level of the 10 and 20 mg doses while the 2.5 mg dose did not.

Kloke et al. (1996) studied cilazapril in patients with varying degrees of renal insufficiency. They compared the effects of a single dose of cilazapril on ACE inhibition over a 4 day period with a 1 mg dose given to NRF patients and a 0.5 mg dose given to IRF patients. The data showed that the duration of inhibition was longer in patients with more severe renal impairment. We simulated these experimental conditions (Fig. 9) and obtained similar observations. The inhibition of ACE for IRF was stronger and lasted longer than for NRF, even with the dose size halved.

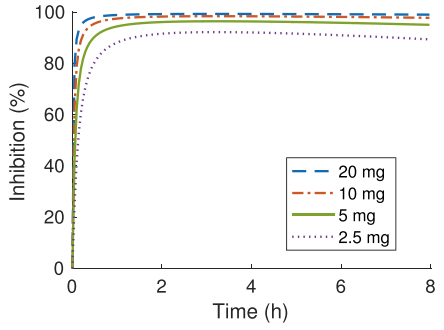

Fig. 8. Cilazapril validation results: inhibition as a function of time for doses of cilazapril for NRF.

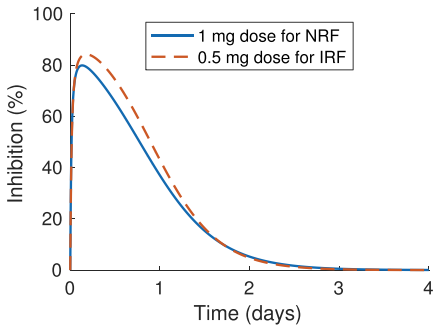

Fig. 9. Cilazapril validation results: inhibition as a function of time for doses of cilazapril: 1 mg for NRF and 0.5 mg for IRF.

3.4. Sensitivity analysis

The local and global sensitivity analysis results for $C_{AI}(2\,h)$, $C_{AII}(2\,h)$, and PRA (2 h) are shown in Figs. 10–12 , respectively. For the output variables C_{AI} and C_{AII} and all four cases, the local sensitivity analysis showed that f was the least sensitive parameter. For PRA, k_R was less sensitive than f (and the other parameters) for both of the benazepril cases. Overall, the parameters for the benazepril IRF case had the smallest local sensitive index values of the cases for C_{AI} and C_{AII}. The local sensitivity index for C_{AII} had the highest average values of the three output variables suggesting that Ang II was the output variable most sensitive to changes in input parameter values.

For all three output variables and all four cases, the global sensitivity analysis showed that f was the least sensitive parameter, confirming the findings from the local sensitivity analysis. Compar-

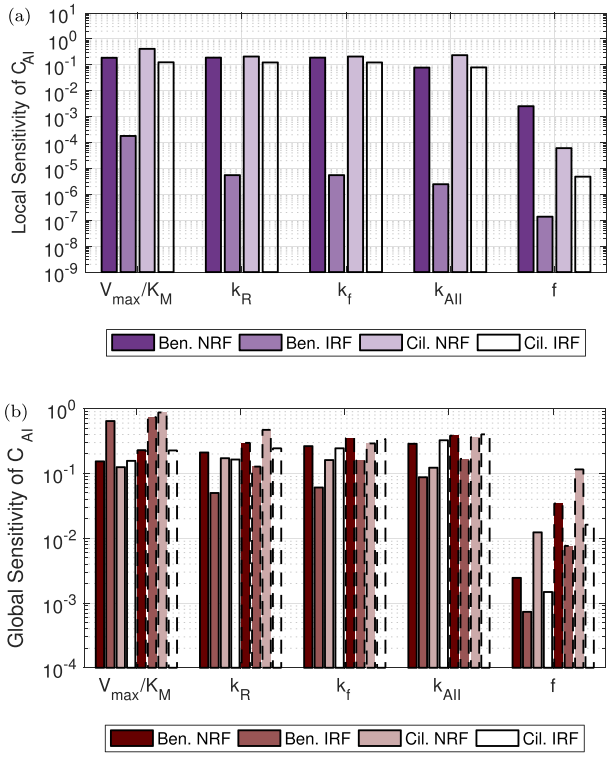

Fig. 10. Ang I concentration sensitivity with respect to the model prediction at 2 h after dosing: (a) local sensitivity analysis and (b) global sensitivity analysis. The drugs benazepril and cilazapril are abbreviated as Ben. and Cil., respectively. In (b) the bars with solid borders are the values of the first-order global sensitivity index S_k with respect to parameter k, and the bars with dashed borders are the values of the total-order global sensitivity index S_{Tk} with respect to parameter k.

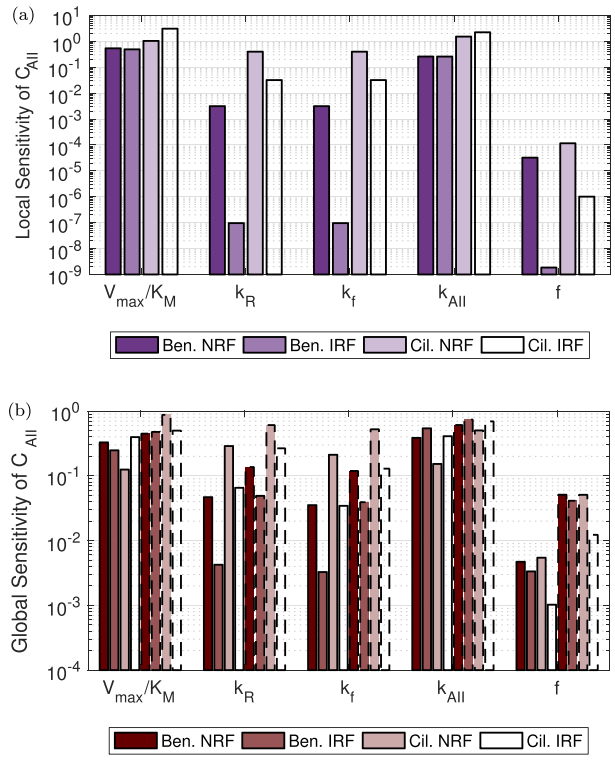

Fig. 11. Ang II concentration sensitivity with respect to the model prediction at 2 h after dosing: (a) local sensitivity analysis and (b) global sensitivity analysis. The drugs benazepril and cilazapril are abbreviated as Ben. and Cil., respectively. In (b) the bars with solid borders are the values of the first-order global sensitivity index S_k with respect to parameter k, and the bars with dashed borders are the values of the total-order global sensitivity index S_{Tk} with respect to parameter k.

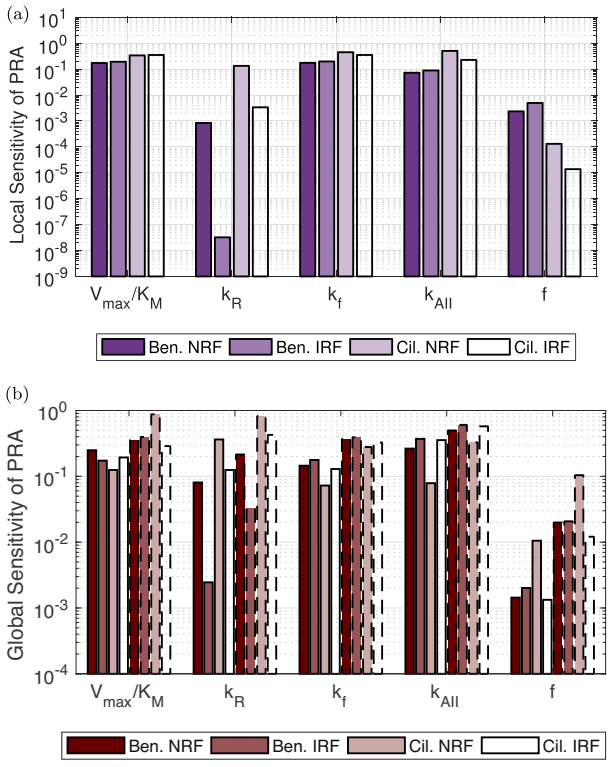

Fig. 12. Plasma renin activity sensitivity with respect to the model prediction at 2 h after dosing: (a) local sensitivity analysis and (b) global sensitivity analysis. The drugs benazepril and cilazapril are abbreviated as Ben. and Cil., respectively. In (b) the bars with solid borders are the values of the first-order global sensitivity index S_k with respect to parameter k, and the bars with dashed borders are the values of the total-order global sensitivity index S_{Tk} with respect to parameter k.

ing the first-order and total-order global sensitivity indices shows that $S_{T_{i,k}} > S_{i,k}$ in all cases. From this comparison, we interpret that the model is non-additive due to nonlinearities and interactions between parameters, as is typical for dynamical systems (Marino et al., 2008).

3.5. General model results

The parameter estimation results showed that distinct sets of parameters were needed to provide the best fits to the four data cases: both benazepril and cilazapril in both NRF and IRF. The PK/PD model was run with the estimated parameter sets and for different magnitudes of single doses daily over a seven-day simulation period to explore the effects of dose size on the levels of diacid form of the drug and Ang II over time in each of the four cases and to make comparisons (Figs. 13 and 14 for benazepril and cilazapril, respectively). Other simulation results (not shown) from the model included inhibition, concentration of Ang I, and PRA. The model also could be used for more frequent dosing intervals (results not shown). The drug dosing magnitudes were chosen to be half and double the dose sizes used for parameter estimation (5 mg for benazepril and 1.25 mg for cilazapril). The concentration for the diacid form of the drug was chosen as a PK result, and the concentration of Ang II was selected as a representative PD result.

It was observed for both drugs that the drug diacid concentration accumulated more rapidly and to a greater extent in IRF than in NRF due to the impaired renal clearance mechanisms. Ang II concentrations were lowered more by larger doses of the same drug, as expected. Note that the Ang II initial condition in each of the four cases was set as the corresponding value in Table 3. For cilazapril, the Ang II dynamics for NRF and IRF were significantly different. The daily minimum of the Ang II concentration at peak

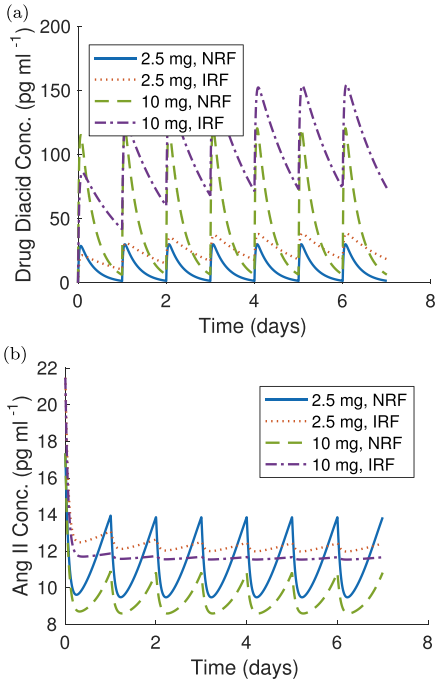

Fig. 13. PK/PD model simulation results for single daily doses of 2.5 mg or 10 mg of benazepril over a seven-day period for normal and impaired renal function. (a) PK result: concentration of the diacid form of the drug and (b) PD result: concentration of Ang II.

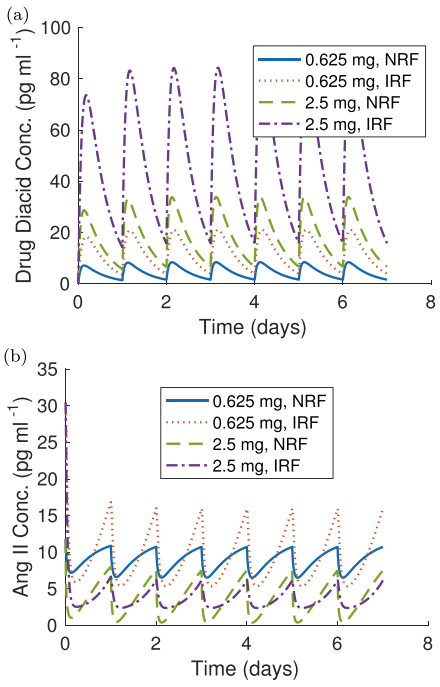

Fig. 14. PK/PD model simulation results for single daily doses of 0.625 mg or 2.5 mg of cilazapril over a seven-day period for normal and impaired renal function. (a) PK result: concentration of the diacid form of the drug and (b) PD result: concentration of Ang II.

therapeutic efficacy was lower for IRF than for NRF, while the duration of therapeutic benefit was shorter for IRF than for NRF. Finally, smaller doses of cilazapril were able to lower the Ang II concentrations substantially more than larger doses of the less potent drug benazepril.

3.6. MATLAB GUI and app

To enable code reuse in research and educational contexts, we created an interactive GUI in MATLAB for manipulating the simulation input and viewing the dynamic model output. The GUI has been packaged as a MATLAB app for ease of distribution. The installation file for the app along with documentation and all of the code to run the model defined in Section 2 with the fitted parameters is provided in a repository at github.com/ashleefv/ACEInhibPKPD (Ford Versypt et al., 2017). The app install file "ACEInhibPKPD.mlappinstall" works much like a zip file with the added features of automated extraction in MATLAB and creation of a menu button to run the GUI. A screenshot of the GUI is shown in Fig. 15. The dose size may have integer or decimal values of less than or equal to 20 mg. The dose frequency can be given integer values from 1 to 24. The drug options are benazepril (drug 1) and cilazapril (drug 2). The kidney function scenarios are normal and impaired. The treatment duration can be set as 1 or 7 days, representing single and consecutive continued dosing. Buttons have been added to the app to run the simulation, plot results, save output plots as png files, and get background information related to an educational design project and ACE inhibitors, specifically the two drugs for this study. The GUI has been used by the authors in a pharmaceutical design project for engineering freshmen (Harrell et al., 2017), a chemical reaction engineering course, and a hands-on simulation demonstration for middle school and high school students. The app install file and the repository also include a MATLAB file titled "run_PKPD_without_GUI.m" that allows users to bypass the use of the GUI to enter the same input as used by the GUI and to display plots of the concentrations of the diacid form of the drug,

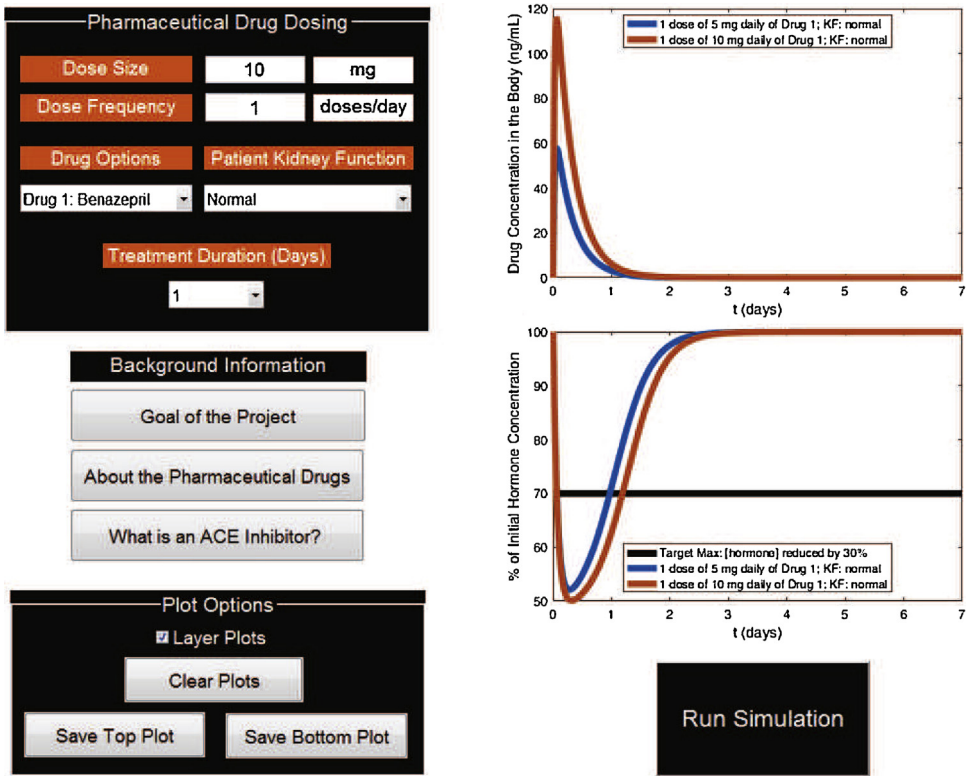

Fig. 15. Interactive MATLAB GUI for design of drug dosing schedules for benazepril and cilazapril for patients with normal and impaired renal function. The drug concentration label refers to the diacid concentration, and "Hormone" is Ang II.

Ang I, and Ang II as well as PRA, inhibition, and the ratio of Ang II to Ang I as functions of time.

4. Conclusions

We have developed a simple physiologically relevant PK/PD model for ACE inhibition parameterized for normal and impaired renal function for two drugs. The model has also been packaged as a MATLAB app to accelerate model reuse by other researchers and/or educators. With the speed of the model solution, the real-life pharmaceutical applications, and the MATLAB GUI, the model can be readily used in educational contexts as a dynamic, interactive visualization tool for learning about biomedical and chemical engineering. The model and results of this work will enable further studies on the impacts of ACE inhibition in disease states such as CKD. In the future, the predictions of systemic hormone levels for Ang I and Ang II could be fed into clinically relevant multiscale models of local tissue effects in microvasculature complications of CKD, diabetes, or hypertension.

Acknowledgments

Funding: This work was supported in part by an Award from Harold Hamm Diabetes Center at the University of Oklahoma Health Sciences Center. The authors would like to thank Prof. Stacey D. Finley for providing the source code for confidence intervals and for technical advice.

References

Ajayi, A.A., Elliott, H.L., Reid, J.L., 1986. The pharmacodynamics and dose-response relationships of the angiotensin converting enzyme inhibitor, cilazapril, in essential hypertension. Br. J. Clin. Pharmacol. 22 (2), 167–175.

Ames, M.K., Atkins, C.E., Lee, S., Lantis, A.C., zumBrunnen, J.R., 2015. Effects of high doses of enalapril and benazepril on the pharmacologically activated renin-angiotensin-aldosterone system in clinically normal dogs. Am. J. Vet. Res. 76 (12), 1041–1050.

Arciero, J.C., Ellwein, L., Ford Versypt, A.N., Makrides, E., Layton, A.T., 2015. Modeling blood flow control in the kidney. In: Jackson, T., Radunskaya, A. (Eds.), Applications of Dynamical Systems in Biology and Medicine. Springer, New York, pp. 55–74.

Asher, J.P., Murray, K.M., 1991. Use of angiotensin-converting-enzyme inhibitors in the management of renal disease. Clin. Pharm. 10 (1), 25–31.

Balfour, J.A., Goa, K.L., 1991. Benazepril: a review of its pharmacodynamic and pharmacokinetic properties, and therapeutic efficacy in hypertension and congestive heart failure. Drugs 42 (3), 511–539.

Brown, N.J., Vaughan, D.E., 1998. Angiotensin-converting enzyme inhibitors. Circulation 97 (14), 1411–1420.

Brown, S.A., Brown, C.A., Jacobs, G., Stiles, J., Hendi, R.S., Wilson, S., 2001. Effects of the angiotensin converting enzyme inhibitor benazepril in cats with induced renal insufficiency. Am. J. Vet. Res. 62 (3), 375–383.

Byers, J.P., Sarver, J.G., 2009. Chapter 10: pharmacokinetic modeling. In: Hacker, M., Bachmann, K., Messer, W. (Eds.), Pharmacology: Principles and Practice. Academic Press, New York, pp. 201–277.

Claasen, K., Willmann, S., Eissing, T., Preusser, T., Block, M., 2013. A detailed physiologically based model to simulate the pharmacokinetics and hormonal pharmacodynamics of enalapril on the circulating endocrine renin-angiotensin-aldosterone system. Front. Physiol. 4 (4), 1–10.

Corbo, J.M., Delellis, T.M., Hill, L.G., Rindfuss, S.L., Nashelsky, J., 2016. ACE inhibitors or ARBs to prevent CKD in patients with microalbuminuria. Am. Fam. Physician 94 (8), 652–653.

Dhillon, S., Kostrzewski, A., 2006. Clinical Pharmacokinetics. Pharmaceutical Press, Chicago.

Ford Versypt, A.N., 2017. ACEInhibPKPD., http://dx.doi.org/10.5281/zenodo.247388 (accessed 17.01.16) http://github.com/ashleefv/ACEInhibPKPD.

Ford Versypt, A.N., Makrides, E., Arciero, J.C., Ellwein, L., Layton, A.T., 2015. Bifurcation study of blood flow control in the kidney. Math. Biosci. 263, 169–179.

Francis, R.J., Brown, A.N., Kler, L., 1987. Pharmacokinetics of the converting enzyme inhibitor cilazapril in normal volunteers and the relationship to enzyme inhibition: development of a mathematical model. J. Cardiovasc. Pharmacol. 9 (1), 32–38.

Gengo, F.M., Brady, E., 1991. The pharmacokinetics of benazepril relative to other ACE inhibitors. Clin. Cardiol. 14 (Suppl. IV), IV-44-50.

Gismondi, R.A.O.C., Oigman, W., Bedirian, R., Pozzobon, C.R., Ladeira, M.C.B., Neves, M.F., 2015. Comparison of benazepril and losartan on endothelial function and vascular stiffness in patients with Type 2 diabetes mellitus and hypertension: a randomized controlled trial. J. Renin-Angiotensin-Aldosterone Syst. 16 (4), 967–974.

Guillaud, F., Hannaert, P., 2010. A computational model of the circulating renin-angiotensin system and blood pressure regulation. Acta Biotheor. 58 (2–3), 143–170.

Guyton, A.C., Coleman, T.G., Granger, H.J., 1972. Circulation: Overall regulation. Ann. Rev. Physiol. 34, 13–46.

Harrell, G.K., McPeak, A.N., Ford Versypt, A.N., 2017. A pharmacokinetic simulation-based module to introduce mass balances and chemical engineering design concepts to engineering freshmen. In: Proceedings of the ASEE Annual Conference, Columbus, OH.

Hong, Y., Dingemanse, J., Mager, D.E., 2008. Pharmacokinetic/pharmacodynamic modeling of renin biomarkers in subjects treated with the renin inhibitor aliskiren. Clin. Pharmcol. Ther. 84 (1), 136–143.

Hoyer, J., Schulte, K.L., Lenz, T., 1993. Clinical pharmacokinetics of angiotensin converting enzyme (ACE) inhibitors in renal failure. Clin. Pharmacokinet. 24 (3), 230–254.

Hsu, T.W., Liu, J.S., Hung, S.C., Kuo, K.L., Chen, Y.C., Hsu, C.C., Tarng, D.C., 2014. Renoprotective effect of renin-angiotensin-aldosterone system blockade in patients with predialysis advanced chronic kidney disease, hypertension, and nnemia. JAMA Intern. Med. 174 (3), 347–354.

Ihler, A., Kernel Density Estimation Toolbox for MATLAB (R13), 2003; http://www.ics.uci.edu/ihler/code/kde.html (accessed 17.01.02).

Jiang, S.Q., Pan, M.L., Wu, S.W., Venners, S.A., Zhong, G.S., Hsu, Y.H., Weinstock, J., Wang, B.Y., Tang, G.F., Liu, D.H., Xu, X.P., 2016. Elevation in total homocysteine levels in Chinese patients with essential hypertension treated with antihypertensive benazepril. Clin. Appl. Thromb.-Hemost. 22 (2), 191–198.

Juillerat, L., Nussberger, J., Menard, J., Mooser, V., Christen, Y., Waeber, B., Graf, P., Brunner, H.R., 1990. Determinants of angiotensin II generation during converting enzyme inhibition. Hypertension 16 (5), 564–572.

Karaaslan, F., Denizhan, Y., Kayserilioglu, A., Gulcur, H.O., 2005. Long-term mathematical model involving renal sympathetic nerve activity, arterial pressure, and sodium excretion. Ann. Biomed. Eng. 33 (11), 1607–1630.

van Kats, J.P., de Lannoy, L.M., Danser, A.H.J., van Meegen, J.R., Verdouw, P.D., Schalekamp, M.A.D.H., 1997. Angiotensin II type 1 (AT_1) receptor-mediated accumulation of angiotensin II in tissues and its intracellular half-life in vivo. Hypertension 30 (1), 42–49.

King, J.N., Panteri, A., Graille, M., Seewald, W., Friton, G., Desavauz, C., 2016. Effect of benazepril, robenacoxib and their combination on glomerular filtration rate in cats. BMC Vet. Res. 12 (124), 1–15.

Kloke, H.J., Ambros, R.J., Van Hamersvelt, H.W., Wetzels, J.F.M., Koene, R.A.P., Huysmans, F.T.M., 1996. Pharmacokinetics and haemodynamic effects of the angiotensin converting enzyme inhibitor cilazapril in hypertensive patients with normal and impaired renal function. Br. J. Clin. Pharmacol. 42 (5), 615–620.

LeBlanc, J.M., Dasta, J.F., Pruchnicki, M.C., Schentag, J.J., 2006. Impact of disease states on the pharmacokinetics and pharmacodynamics of angiotensin-converting enzyme inhibitors. J. Clin. Pharmacol. 46 (9), 968–980.

Lo, A., Beh, J., De Leon, H., Hallow, M.K., Ramakrishna, R., Rodrigo, M., Sarkar, A., Sarangapani, R., Georgieva, A., 2011. Using a systems biology approach to explore hypotheses underlying clinical diversity of the renin angiotensin system and the response to antihypertensive therapies. In: Kimko, H.H.C., Peck, C.C. (Eds.), Clinical Trial Simulations. Springer, New York, pp. 457–482.

Marino, S., Hogue, I.B., Ray, C.J., Kirschner, D.E., 2008. A methodology for performing global uncertainty and sensitivity analysis in systems biology. J. Theor. Biol. 254 (1), 178–196.

McKay, M.D., Beckman, R.J., Conover, W.J., 1979. A comparison of three methods for selecting values of input variables in the analysis of output from a computer code. Technometrics 21 (2), 239–245.

Morimoto, K., Matsunaga, M., Hara, A., Kawai, C., 1980. Studies on the activation and molecular weight of inactive renin in human plasma. Hypertension 2 (5), 680–685.

Niu, H., Nie, L., Liu, M., Chi, Y., Zhang, T., Li, Y., 2014. Benazepril affects integrin-linked kinase and smooth muscle α-actin expression in diabetic rat glomerulus and cultured mesangial cells. BMC Nephrol. 15 (135), 1–10.

Noda, T., Yaginuma, T., O'Rourke, M.F., Hosoda, S., 2006. Effects of nifedipine on systemic and pulmonary vascular impedance in subjects undergoing cardiac catheterization. Hypertens. Res. 29 (7), 505–513.

Oates, H.F., Fretten, J.A., Stokes, G.S., 1974. Disappearance rate of circulating renin after bilateral nephrectomy in the rat. Clin. Exp. Pharmacol. Physiol. 1 (6), 547–549.

Ramusovic, S., Laeer, S., 2012. An integrated physiology-based model for the interaction of RAA system biomarkers with drugs. J. Cardiovasc. Pharmcol. 60 (5), 417–428.

Schaller, M.D., Nussberger, J., Waeber, B., Bussien, J.P., Turini, G.A., Brunner, H., Brunner, H.R., 1985. Haemodynamic and pharmacological effects of the converting enzyme inhibitor CGS 14824A in normal volunteers. Eur. J. Clin. Pharmacol. 28 (3), 267–272.

Sent, U., Gossl, R., Elliott, J., Syme, H.M., Zimmering, T., 2015. Comparison of efficacy of long-term oral treatment with telmisartan and benazepril in cats with chronic kidney disease. J. Vet. Intern. Med. 29 (6), 1479–1487.

Shionoiri, H., Gotoh, E., Takagi, N., Takeda, K., Yabana, M., Kaneko, Y., 1988. Antihypertensive effects and pharmacokinetics of single and consecutive doses of cilazapril in hypertensive patients with normal and impaired renal function. J. Cardiovasc. Pharmacol. 11 (2), 242–249.

Shionoiri, H., Ueda, S., Minamisawa, K., Minamisawa, M., Takasaki, I., Sugimoto, K., Gotoh, E., Ishii, M., 1992. Pharmacokinetics and pharmacodynamics of benazepril in hypertensive patients with normal and impaired renal function. J. Cardiovasc. Pharmacol. 20 (3), 348–357.

SourceForge, 2015. Plot Digitizer (accessed 17.01.02) http://plotdigitizer.sourceforge.net/.

Toutain, P.L., Lefebvre, H.P., 2004. Pharmacokinetics and pharmacokinetic/pharmacodynamic relationships for angiotensin-converting enzyme inhibitors. J. Vet. Pharmacol. Ther. 27 (6), 515–525.

Wang, Y., Xiao, J., Suzek, T.O., Zhang, J., Wang, J., Zhou, Z., Han, L., Karapetyan, K., Dracheva, S., Shoemaker, B.A., Bolton, E., Gindulyte, A., Bryant, S.H., 2012. PubChem's bioassay database. Nucleic Acids Res. 40 (D1), D400–D412.

Yamout, H., Lazich, I., Bakris, G.L., 2014. Blood pressure, hypertension, RAAS blockade, and drug therapy in diabetic kidney disease. Adv. Chronic Kidney Dis. 21 (3), 281–286.

Zhang, Q., Ji, Y.Q., Lv, W., He, T.W., Wang, J.P., 2016. Protective effects of leflunomide on renal lesions in a rat model of diabetic nephropathy. Ren. Fail. 38 (1), 124–130.

Zhang, X.Y., Trame, M.N., Lesko, L.J., Schmidt, S., 2015. Sobol sensitivity analysis: a tool to guide the development and evaluation of systems pharmacology models. CPT Pharmacomet. Syst. Pharmacol. 4 (2), 69–79.